

Effect of Melting Pool on the Residual Stress of Welded Structures in Finite Element Analysis

Jang Hyun Lee¹, Se Yun Hwang² and Yong Sik Yang¹

¹ Department of Naval Architecture and Ocean Engineering, Inha University, Incheon, Korea

² Department of Naval Architecture and Ocean Engineering, Inha University Graduate School, Incheon, Korea;

Corresponding Author: jh_lee@inha.ac.kr

Abstract

Welding processes cause undesirable problems, such as residual stresses and deformations due to the thermal loads imposed by local heating, melting, and cooling processes. This paper presents a computational modeling technique to simulate the Gas Metal Arc Welding (GMAW) process, emphasizing the effect of the melting bead on the residual stress distribution. Both a three-bar analogy and a three-dimensional thermo-mechanical finite element analysis are carried out in order to explain the effect. Element (de)activation, enthalpy, and adjustment of the reference temperature of thermal strain are considered with respect to the effect of the weld filler metal added to the base metal during a thermo-elastic-plastic analysis. Stress distributions obtained by the present study are compared with measured values and available data from other studies. The effect of the melting bead on the residual stress distribution is discussed and demonstrated.

Keywords: residual stresses, GMAW, welding, thermo-elastic-plastic, finite element analysis, weld bead

1 Introduction

Residual stresses are generated in a welding process because of local heating, a high temperature bead, and rapid cooling. There has been increasing use of FEA (Finite Element Analysis) procedures to predict the residual stresses since it is difficult to directly measure the stresses. Recently, with advances in numerical simulations, three-dimensional FEA has been widely used the moving heat input, nonlinear material properties, temperature-dependent convective heat transfer, and radiation in the welding process.

Masubuchi(1980) suggested a logical process to explain the residual stresses, stating that the value of longitudinal stress reaches a peak value in the middle of the joint and decreases along the width direction. However, many experimental studies (Sorenson 1999, Zhu and Chao 2002, Kim 2000, Lee 1995) show that the residual stress in the middle of the joint does not reach a peak value.

Present study seeks to find a qualitative clue that can explain the pattern of residual stresses obtained by measurement. The physical process of phase transformation (melting

and solidification) of the weld bead, the history of thermal strains, and the deposited bead at the melting temperature are considered in the analysis of residual stresses. In order to find a reasonable method to explain the decreasing stress at the middle of the welding line, three-bar models and a 3-dimensional FEA model of the butt-joint are discussed by two case-studies. Element (de)activation, enthalpy, and adjustment of reference temperature in thermal strains are considered in the suggested FEA models.

2 Three-bar Analogy for Residual Stress

To investigate the quantitative characteristics of the weld bead, an example of a three-bar model is examined (Cheng 1995). It consists of a middle bar, two side bars, and end-constraints. The most significant effect of the melting bead is free thermal strain. When filler metal is deposited at melting temperature, it makes its thermal strain be free. The reference temperature (T_{ref}) for the thermal strain is set at the melting temperature so that the free thermal strain can be taken into account. In this section, two test cases are considered as described in Table 1.

Table 1: Parameters of case studies

	Case1	Case2
Temperature history[°C]	0→500→0	500→0
T_{ref} [°C]	0	500

The change of temperature makes the variation of Young's modules, yield stress, and thermal expansion coefficient. Variation of material properties with temperature is considered in the analysis. The material in its plastic behavior is assumed as the elastic perfectly plastic material. To include the temperature-dependent material properties, which are suggested by Lee(1995) and Kim(2000) are used in the finite element model (Figure 1~ Figure 6).

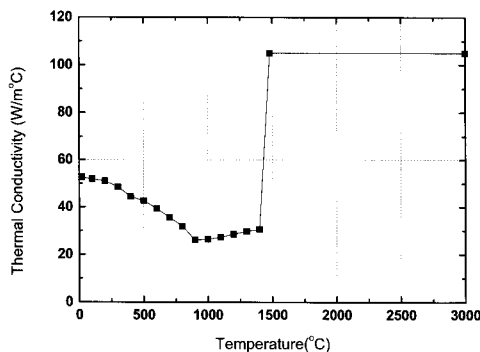


Figure 1: Thermal conductivity

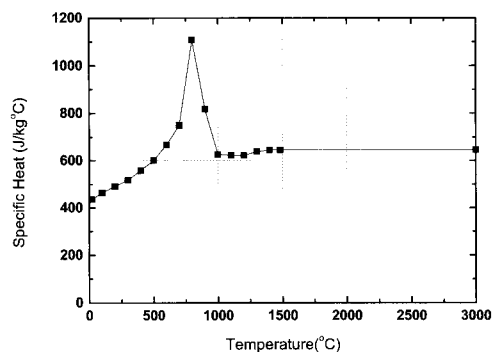


Figure 2: Specific heat

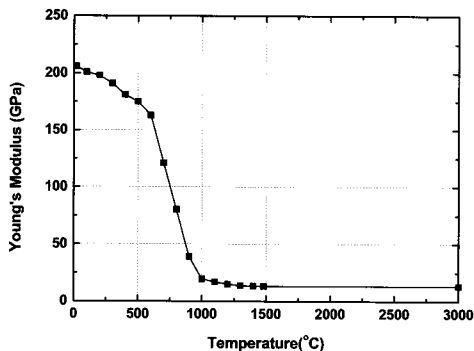


Figure 3: Elastic modulus

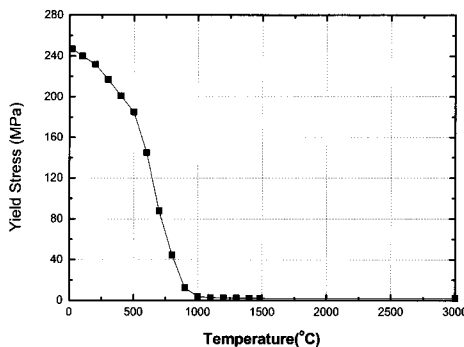


Figure 4: Yield stress

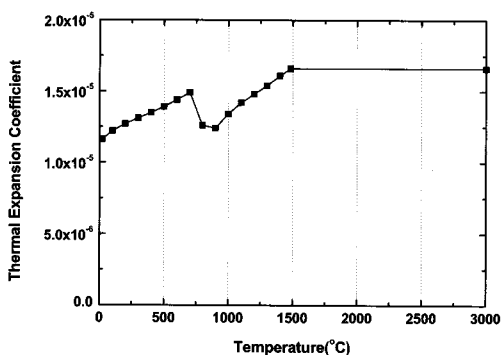


Figure 5: Thermal expansion coefficient

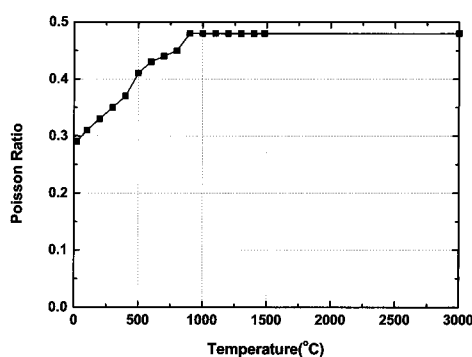


Figure 6: Poisson ratio

The calculation was performed with the model with the dimension as follows. Two side-bars are assumed to have room temperature.

The section area of the central bar, $A_c = 0.01 [m^2]$

The section area of the side-bar, $A_s = 0.04 [m^2]$

In Case 1, compressive force takes place from the beginning, and the compressive stress approaches the yield value as the temperature is heightened. In the cooling phase after the heating phase, the central bar undergoes shrinkage and tension is invoked by the strength of the side-bars. In Case 2, the central bar undergoes thermal contraction since the temperature cools down from 500°C to room temperature. Figure 7 shows the stress history in the central bar with respect to the temperature for Cases 1 and 2. σ_c (Stress of central bar) in Case 2 increases since the central bar endures only a contraction process that is resisted by the side bars. It can be concluded that the history of residual stress is different from that described in traditional theory suggested by Masubuchi(1980).

Figure 7 shows the history of strains in case that the center experiences the heating and cooling cycle. As the central bar undergoes the heating (up to 500°C) and cooling (to 0°C), the two side-bars act as the elastic body that resists against the deformation of the central bar. The central bar has the elastic deformation in relatively low temperature. It takes the compression, and the compression approaches to the yielding stress as the temperature got heightened. The deformation is determined in the equilibrium, constitutive and compatibility equations. In the cooling phase after the heating phase that makes the maximum temperature, the central bar undergoes the shrinkage and has the tension

invoked by the strength of the side-bars. As the temperature goes down, the tension reaches the plastic stress. The plastic behavior makes the residual strain. Figure 8 shows the history of axial strains of each bar in case that the initial temperature of the central bar starts with 500°C. The central bar undergoes the thermal contraction since the temperature of the central bar cools down from 500°C to room temperature. Therefore the axial stress of the central bar increases as the temperature cools down as shown in Figure 8. Therefore the residual stresses of two cases are compared in the Figure 9.

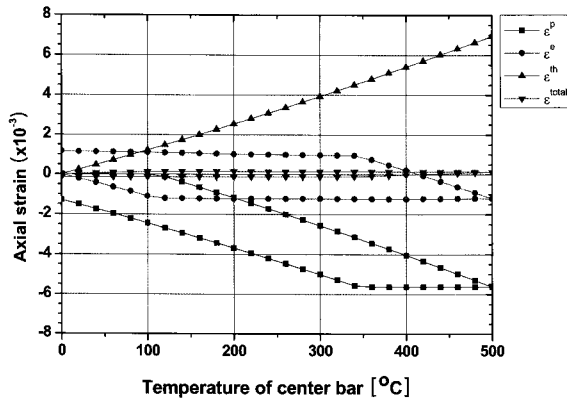


Figure 7: Strain history of center bar (Case1)

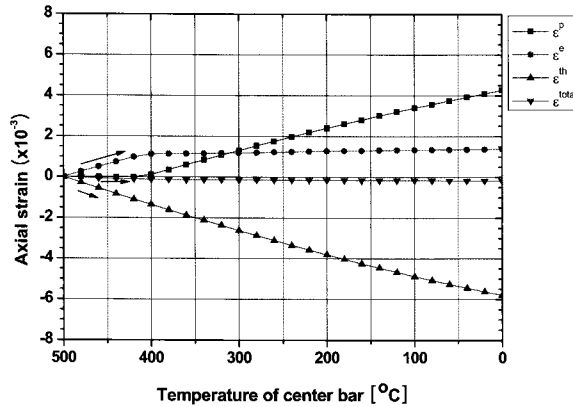


Figure 8: Strain history of side bars (Case2)

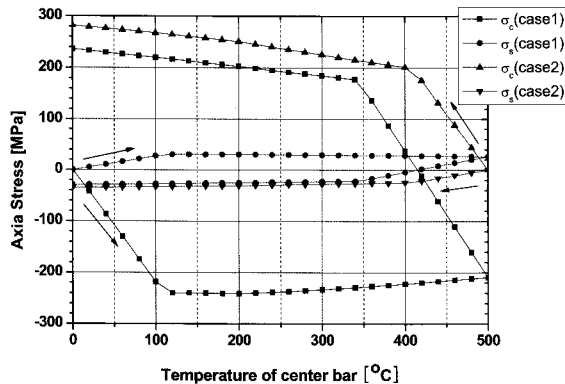


Figure 9: History of axial stresses in each bar

3 Three-Dimensional Finite Element Model

An uncoupled heat transfer and thermo-elasto plastic analysis is applied to the three-dimensional finite element model to investigate the effect of melting pool on the residual stress. The transient temperature distributions are loaded as boundary condition in the subsequent thermo-elastic-plastic analysis.

3.1 Thermal mechanical analysis

Temperature field in the work pieces is determined by the heat diffusion equation.

$$\nabla \cdot (k \nabla T) + q^v = \rho C \dot{T} \quad (1)$$

where, k is the heat conductivity, T is the temperature, q^v is the internal heat generation rate, ρ is the density and C is the specific heat capacity of the material. The heat introduced to the base metal consists of the heat energy transferred from the arc and the latent heat energy from the filler metal. The heat energy of the arc can be modeled by the heat flux (q'') (Tekriwal 1989).

$$q'' = \frac{\eta_a VI}{\pi r_b^2} e^{-3\left(\frac{r}{r_b}\right)^2} \quad (2)$$

where η_a is the arc efficiency, r is the position of the weld torch in the welding line direction, r_b is the arc beam radius, V and I are the arc voltage and current, respectively. The convective heat dissipation of the ambient air and the radiative heat dissipation are modeled by the equation suggested by Patel(1985).

$$q_n = 24.1 \times 10^{-4} \varepsilon^r T^{1.41} (T - T_a) \quad (3)$$

where q_n is the heat flux, ε^r is the hemispherical emissivity, T the surface temperature of the workpiece, and T_a the ambient temperature. The heat diffusion equation can be formulated by a finite element formulation. Newton-Raphson and PCG (Pre-conditioned Conjugate Gradient) iterative method are used to solve the finite element formula. The Crank-Nicolson integration scheme is adopted to obtain the transient temperature.

The thermal stress and strain are computed using the temperature-dependent material properties of thermal expansion, Young's modulus, yield stress, and plastic modulus. For the plastic strain, a rate-independent plastic model is adopted. The Von Mises yield condition, temperature-dependent material properties, and linear isotropic hardening model are adopted in the computation procedure. The stress ratio of the thermo-elastic-plastic material may be characterized by the following incremental constitutive equation (Lee 1999):

$$\dot{\sigma}_{ij} = C_{ijkl} (\dot{\varepsilon}_{kl} - \dot{\varepsilon}_{kl}^{th} - \dot{\varepsilon}_{kl}^{pl}) + d_{ij} \dot{T} \quad (4)$$

where σ_{ij} are stresses, C_{ijkl} are material parameters, which are related to the generalized Hooke's law for elastic materials, ε_{ij} are total strains, ε_{ij}^{th} are thermal strains, and ε_{ij}^{pl} are plastic strains. d_{ij} is defined as $d_{ij} = dC_{ijkl} / dT C_{klmn}^{-1} \sigma_{mn}$.

3.2 Welding Bead Deposition

3.2.1 Phase Transformation

The location of the liquidus and solidus temperatures is of great importance in welding since melting and solidification of the weld bead are included in bead area. To include the phase change, the latent heat must be considered. To account for the latent heat, the enthalpy of the material as a function of temperature is considered, as shown in Figure 10.

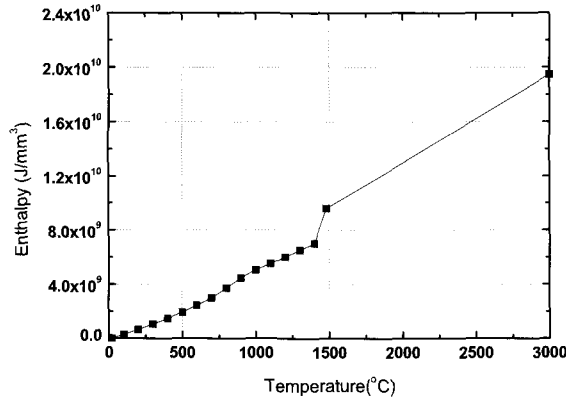


Figure 10: Enthalpy vs. temperature curve

3.2.2 Filler Metal Deposition and Element Activation

To model the deposition of the weld filler metal, ‘element activation and deactivation’, provided by ANSYS, is adopted. Element deactivation is implemented by multiplying its stiffness by a very small number and by removing its mass from the overall mass matrix. A deactivated element remains in the model but contributes a near-zero stiffness (or conductivity etc.) value to the overall matrix. The element may be reactivated by recovering the stiffness according to the location of rods of the filler metal (Kim 2000).

3.2.3 Thermal stress free in melting state

For welding processes that involve a phase change of the filler metal, Eq. (5) is used to derive the thermal strain for temperature T .

$$\epsilon^{th} = \alpha(T - T_{ref}) \quad (5)$$

where α is the heat expansion coefficient. During welding, the bead introduced from a weld rod has a temperature history that is different from that of the workpiece, because it experiences only contraction by cooling whereas the workpiece goes through both expansion and contraction. To solve this inconsistency in the temperature histories, two different reference temperatures, for the bead and the workpiece, must be applied in Eq. (5). For the workpiece, the room temperature is selected as its reference temperature. Since the incoming bead is assumed to be at a temperature of more than 2000°C, it begins to change its state from liquidus to solidus and transfers its thermal energy to the workpiece.

Therefore, at the moment of binding, the bead possesses neither stress nor initial thermal strain.

3.2.4 Cut off temperature

Mechanical properties of the welding material, such as Young's modulus, yield stress, and plastic modulus, decrease significantly as the temperature approaches the melting point. Therefore, 1500°C is used as the cut-off temperature (T_{cut}), above which the stress behavior is assumed to be negligible (Zhu 2000). The Newton-Raphson method was used in each time-step, and the Frontal method was used to solve the equilibrium matrix during the FEA procedure.

3.3 Numerical examples

For convenience, GMAW, this is suggested by Kim(2000) and Lee(1995), is modeled through the finite element model. The GMAW butt joint of plates has been investigated for testing the effect of the melting bead. The temperature distribution and stress distribution obtained during the present study are compared with the results available from Lee(1995). Typical parameters of GMAW are given in Table 2. For comparison, two cases are considered in this section, as shown in Table 3.

Table 2: Parameters of welding

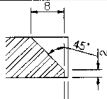
Parameter	Value
Length:80mm Width:150 mm Thickness: 10 mm	
Filler metal temperature	2000 °C
Total arc efficiency	0.67
Traveling speed	2 mm/sec
Arc efficiency	0.40
Effective arc radius	8 mm
Welding voltage / current	28 V / 220 A

Table 3: Parameters of case studies

	Case1	Case2
Filler metal generation	None	Yes
T_{ref} of Filler metal [°C]	Room	T_{cut}
T_{ref} of Workpiece [°C]	Room	Room

This section explains the numerical results of residual stress for the two cases. FEA results are compared with the experimental data obtained from Lee(1995). Accordingly, the effect of melting filler metal on residual stresses is discussed. Figure 11 shows the temperature distribution during the welding process of Case 2 obtained by finite element analysis.

Figure 12 shows another profile of residual stress measured by Sorenson(1999). The curve ‘ $-\sigma_x$ (Masubuchi)’ and curve ‘x’ show the results of Masubuchi(1980) and those of the measurement presented by Sorenson(1999), respectively.

The distribution of residual stress in the longitudinal direction, σ_{xx} , along the middle section for Case 1 and Case 2 is illustrated in Figure 13. The residual stress measured by Lee(1995) is also shown in Figure 14. The result of Case 2 is similar to the measured data. The residual stress is in good agreement with that of the experiment except in the area close to the weld line.

Figure 15 and Figure 16 shows the residual stresses along the middle section of the workpiece for Case 1 and Case 2, respectively. Stress pattern of Figure 15, which does not consider the melting pool, can't explain the crater pattern of stress distribution. The crater pattern of σ_x in Figure 16 is similar to the pattern obtained by Figure 12, which considers the free thermal strain and bead deposition. Since the welding conditions of Case 2 are different from those of Sorenson(1999), the peak value of residual stress is not consistent. However, the effect of the melting bead can explain the crater pattern of stress distribution near the weld center line.

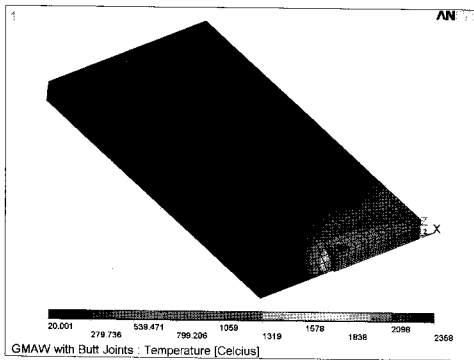


Figure 11: Temperature distribution (Case 2)

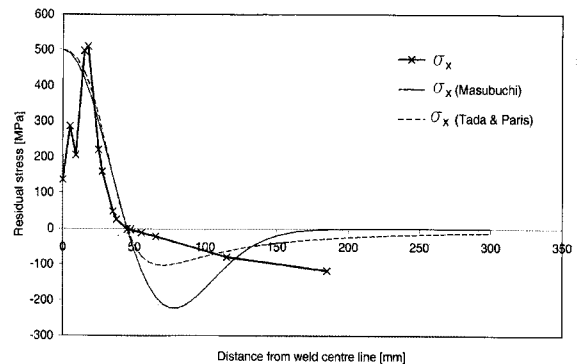


Figure 12: Typical shape of residual stress from Sorenson(1999)

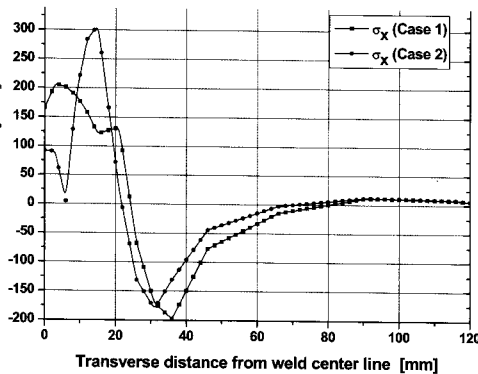


Figure 13: Comparison of residual stress (σ_{xx}) distribution in each case

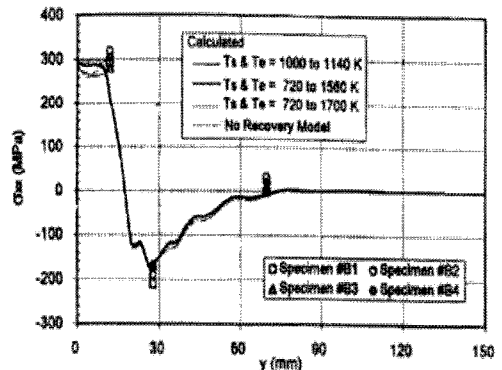


Figure 14: Residual stress (σ_{xx}) distribution from Lee(2000)

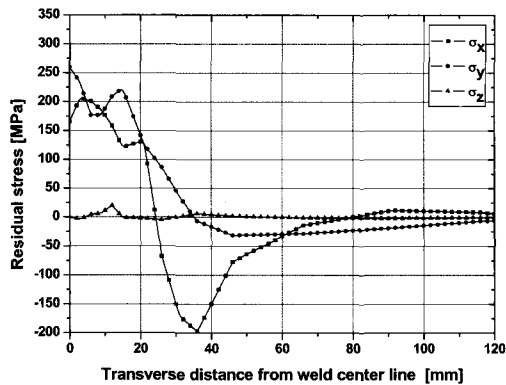


Figure 15: Residual stresses along transverse direction (Case 1)

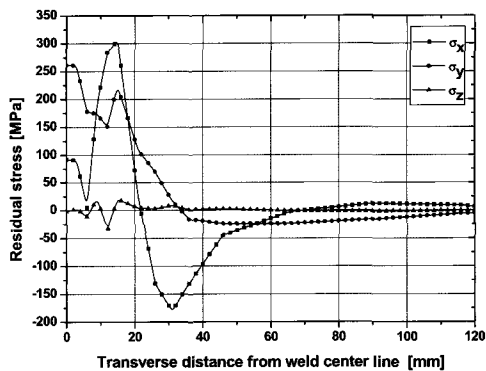


Figure 16: Residual stresses along transverse direction (Case 2)

4 Discussion

To investigate the effect of the melting bead on residual stress in a numerical simulation of a welding process, a 3-bar model and a detailed 3D thermo-mechanical analysis are performed. Two sets of case studies are performed considering the free thermal strain and element deposition of filler metal in the melting state. Numerical results are compared with experimental data provided by other researchers. From the present studies, it is shown not only that the melting bead has a significant effect on the residual stress profile, but also that free thermal-strain and activation of filler metal can account for the peak stress which is decreasing in the weld center line.

References

- ANSYS. 2005. Advanced Analysis Techniques Guide. ANSYS, Inc.
- Cheng, W. 2005. In-plane Shrinkage Strains and Their Effects on Welding Distortion in Thin-wall Structures, Ph.D. Thesis, Ohio State University
- Lee, D.W. 1995. Thermo-Elasto-Plastic Modeling of GMAW Using the Finite Element Method, Ph.D. Thesis, Seoul National University.
- Lee, J.H. 1999. Relation between Input Parameters and Residual Deformations in Line Heating Process Using Finite Element Method and Multi-Variate Analysis. Ph.D. Thesis, Seoul National University.
- Kim, J.H. 2000. Simulation of GMAW using 3-Dimensional Thermo-elasto-plastic Analysis. M.Sc. Thesis, Seoul National University.
- Masubuchi, K. 1980. Analysis of Welded Structures. Pergamon Press, Oxford, New York.
- Patel, B.G. 1985. Thermo-elasto-plastic Finite Element Formulation for Deformation and Residual Stresses Due to Welds. Ph.D. Thesis, Carleton University
- Sorenson, M.B. 1999. Simulation of Welding Distortions in Ship Section. Ph.D. Thesis, Technical University of Denmark.
- Tekriwal, P.K. 1989. Three-dimensional Transient Thermo-elasto-plastic Modeling of Gas Metal Arc Welding using The Finite Element Method. Ph.D. Thesis, University of Illinois at Urbana-Champaign.

J. H. Lee et al: Effect of Melting Pool on the Residual Stress ...

Zhu, X.K. and Y.J. Chao. 2002. Effects of Temperature-dependent Material Properties On Welding Simulation. *Computers & Structures*, **80**, 11, 967-976.